

Genetic Contributions to Regional Variability in Human Brain Structure: Methods and Preliminary Results

I. C. Wright,* P. Sham,* R. M. Murray,* D. R. Weinberger,† and E. T. Bullmore*‡

*Institute of Psychiatry, King's College London, London, United Kingdom; †National Institute of Mental Health, National Institutes of Health, Bethesda, Maryland; and ‡Department of Psychiatry, University of Cambridge, Cambridge, United Kingdom

Received July 24, 2001

Twin studies provide one approach for investigating and partitioning genetic and environmental contributions to phenotypic variability in human brain structure. Previous twin studies have found that cerebral volume, hemispheric volume, ventricular volume, and cortical gyral pattern variability were heritable. We investigated the contributions of genetic and environmental factors to both global (brain volume and lateral ventricular volume) and regional (parcellated gray matter) variability in brain structure. We examined MR images from 10 pairs of healthy monozygotic and 10 pairs of same-sex dizygotic twins. Regional gray matter volume was estimated by automated image segmentation, transformation to standard space, and parcellation using a digital atlas. Heritability was estimated by path analysis. Estimated heritability for brain volume variability was high (0.66; 95% confidence interval 0.17, 1.0) but the major effects on lateral ventricular volume variability were common and unique environmental factors. We constructed a map of regional brain heritability and found large genetic effects shared in common between several bilateral brain regions, particularly paralimbic structures and temporal-parietal neocortex. We tested three specific hypotheses with regard to the genetic control of brain variability: (i) that the strength of the genetic effect is related to gyral ontogenesis, (ii) that there is greater genetic control of left than of right hemisphere variability, and (iii) that random or fluctuating asymmetry in bilateral structures is not heritable. We found no evidence in support of the first two hypotheses, but our results were consistent with the third hypothesis. Finally, we used principal component (PC) analysis of the genetic correlation matrix, to identify systems of anatomically distributed gray matter regions which shared major genetic effects in common. Frontal and parietal neocortical areas loaded positively on the first PC; some paralimbic and limbic areas loaded negatively. Bilateral insula, some frontal regions, and temporal neocortical regions functionally specialized for audition and language loaded strongly on the second PC. We conclude that large samples are required for powerful investigation of genetic effects in imag-

ing data from twins. However, these preliminary results suggest that genetic effects on structure of the human brain are regionally variable and predominantly symmetric in paralimbic structures and lateral temporal cortex. © 2002 Elsevier Science (USA)

Key Words: brain anatomy; twins; genetic correlation matrix; heritability; asymmetry; MRI; path analysis; structural equation modeling.

INTRODUCTION

Brain structure varies between individuals in cerebral volume, ventricular volume, sulcal-gyral patterns, and volumes of cortical and subcortical subregions. What factors control this variability and how do these factors interrelate? The sources of variability may be broadly partitioned into genetic and environmental contributions. While brain development is directly controlled by a large number of genes (Weickert and Weinberger, 1998), it is also subject to a variety of environmental influences (such as nutrition and the intrauterine environment). The effects of environmental factors may also be modulated by interaction with genes.

Twin studies provide a method to investigate genetic and environmental contributions to phenotypic variability. Whereas monozygotic twins have identical genotypes, dizygotic twins share only 50% of their genotype on average, permitting quantitative assessment of the genetic contribution to the phenotype (subject to a number of important assumptions detailed below). Previous twin studies have found that cerebral volume, hemispheric volume (Bartley *et al.*, 1997), and ventricular volume (Reveley *et al.*, 1982) were highly heritable. Bartley *et al.* (1997) also found that cortical gyral patterns were heritable, but to a lesser degree than cerebral volume.

In this study we have extended this work by investigating (i) the interrelationship between the genetic and the environmental contributions to brain volume and lateral ventricular volume and (ii) the heritability

of regional gray matter, after parcellation of cerebral gray matter into cortical regions corresponding approximately to Brodmann's areas and other major brain regions. Lohmann *et al.* (1999) have argued that the shape of deep (ontogenetically early) sulci of the human brain is more strongly predetermined than that of superficial sulci. Here we have tested the related hypothesis (iii) that regional heritability is correlated with ontogenesis, such that the structures which develop earliest are the most genetically controlled. We have also investigated (iv) genetic effects on symmetric and asymmetric brain development and finally (v) we have used principal components analysis of the "genetic correlation matrix" to identify supraregional brain systems which share major genetic contributions to heritability.

These investigations necessarily entailed using some statistical concepts and tools which we will informally introduce here; more detailed description is provided under Subjects and Methods and in the cited references.

The key statistical technique is path analysis, also often referred to as structural equation modeling. Path analysis was originally developed by the biometrician Sewall Wright, between 1918 and 1934 approximately, and has been widely used for analysis of multivariate data in social, political, and behavioral sciences following the introduction of computer packages such as LISREL in the 1970s (see Bollen (1989) for historical and statistical background).

Path analysis starts from a set of correlations or covariances empirically estimated between each pair of a set of variables. If there are p variables, these pairwise correlations or covariances can be tabulated in a symmetric ($p \times p$) correlation or covariance matrix. Simply looking at such a correlation matrix may tell us something about the patterns of association between variables: we may note for example that the correlations $r(\alpha, \beta)$, $r(\beta, \gamma)$, and $r(\alpha, \gamma)$ are all large and positive, suggesting that the variables α , β , and γ are elements of an integrated or connected system. However, because correlation coefficients are symmetric, i.e., $r(\alpha, \beta) = r(\beta, \alpha)$, correlational analysis alone cannot inform us about *causal* or unidirectional relationships between variables. Wright's contribution was to define a set of rules that could be used to transform a set of empirically estimated correlation coefficients into a (generally smaller) set of so-called *path coefficients* that quantify the unidirectional relationships between variables allowed by a prior *path model*. Path analysis can therefore be approximately understood as a way of converting correlation coefficients to partial regression coefficients.¹

¹ Equivalently, in the terminology of functional brain imaging, path analysis has been used to translate measures of functional connectivity to measures of effective connectivity between brain regions in a neurocognitive network; see Bullmore *et al.* (2000).

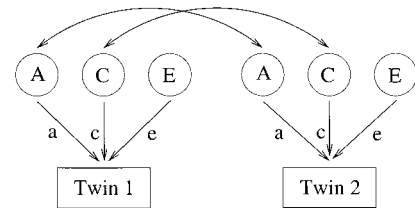


FIG. 1. Path diagram for univariate ACE model. A, C, and E are latent variables with an influence on manifest brain structure. A, additive genetic effects; C, common (shared) environmental effects; E, nonshared environmental effects. The size of each of these effects on phenotypic variability is quantified by the path coefficients a , c , and e , respectively. The proportion of total variance accounted for by each effect is the square of the corresponding path coefficient; i.e., heritability = a^2 . The model assumes that correlation between additive genetic effects is 1.0 for MZ twin pairs and 0.5 for DZ twin pairs.

An important generalization of Wright's basic method is to incorporate latent variables or factors in the path model. This means that the empirical correlations between a set of manifest variables may be modeled not only in terms of causal interaction between the manifest variables themselves but also in terms of causal effects of latent variables on manifest variables. In this more general sense, path analysis is formally very similar to confirmatory factor analysis (see Loehlin (1987) for a general introduction to latent variable models).

In path analysis of data from twin studies, one generally starts from the correlation(s) between twins on one (or more) phenotypic characteristic(s). Simply comparing the twin-pair correlations separately estimated for monozygotic (MZ) and dizygotic (DZ) twins might indicate that the variable in question is more highly correlated between MZ pairs than between DZ pairs, immediately suggesting that variability in this characteristic is genetically determined to a large extent (Thompson *et al.*, 2001). However, there may be many nongenetic contributions to variability that are shared between MZ twins and it is important to disambiguate these shared environmental effects from additive genetic effects on empirical covariation. A path model for causal effects of additive genetic (A), common environmental (C), and nonshared environmental or "error" (E) latent factors on phenotypic variability can be written diagrammatically using the convention that the unidirectional effect of a factor A on a regional variable β is represented as a single-headed arrow pointing from A to β (see Fig. 1). The path coefficients quantifying these effects can then be estimated from the MZ and DZ correlation matrices, assuming that genetic effects will be 100% correlated in MZ twin pairs and 50% correlated in DZ pairs (correlations are diagrammatically represented as double-headed arrows in the path diagram of the ACE model shown in Fig. 1). The percentage of variability in a region accounted for by a

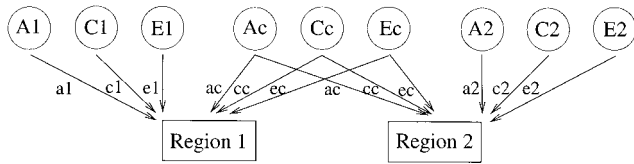


FIG. 2. Path diagram for bivariate ACE model. A1, C1, E1 is a set of specific factors influencing variability only of region 1; A2, C2, E2 is a set of specific factors influencing variability only of region 2; Ac, Cc, Ec is a set of common factors influencing variability of both regions. A, additive genetic effects; C, common environmental effects; E, nonshared environmental effects. The model is identified under the constraint that the path coefficients for the common effects are identical for both regions. If region 1 and region 2 are bilaterally homologous regions, then the size of the common effects on variability measures genetic and environmental effects on symmetric brain structure.

particular factor is the square of the corresponding path coefficient. Thus the *heritability*, or percentage of variability accounted for by the additive genetic factor A, is simply estimated by a^2 .

This basic model can be elaborated by considering more than one phenotypic characteristic. We will refer to the simpler case, where only one phenotypic variable is modeled, as a *univariate* path analysis. Then, in a *bivariate* analysis, we consider two phenotypic variables simultaneously and specify a path model that includes genetic and environmental effects on each variable specifically and genetic and environmental effects that are common to both variables (Fig. 2). If the two variables are homologous brain regions in the right and left hemispheres, then estimation of common genetic factors is an analysis of genetic effects on *symmetric* brain structure. We can also approach the question of genetic effects on lateralized or asymmetric brain structure by deriving a *laterality index* from a homologous pair of regional measurements, e.g., right and left superior temporal gyrus, and using this laterality index as the dependent variable in a univariate path analysis. Later we formally define and use an index of *fluctuating asymmetry*, which refers to left-right differences in bilaterally homologous structures that may fluctuate in magnitude from one individual to another and are therefore generally regarded indicative of random “developmental noise.”

The last set of statistical ideas that we need to introduce is the use of *principal component (PC) analysis* to decompose the *genetic correlation matrix* (Kingsolver and Wiernasz, 1991). To estimate the genetic correlation between a pair of brain regions, we first fit a bivariate path model (as in Fig. 2) with both regional measurements treated as dependent phenotypic characteristics. This will provide estimates of the heritability common to both structures and the heritability specific to each structure. The genetic correlation coefficient is then simply defined as the ratio of common heritability of the two structures to their total herita-

bility (see Eq. (3)); in other words, the genetic correlation coefficient is the proportion of their total heritability that is shared in common between the two genetically correlated regions. Estimating this coefficient for each pair of regions will result in a symmetric genetic correlation matrix. Direct inspection of this matrix will reveal regional pairs which have proportionally large genetic effects in common; but because the matrix may be large, we can use principal component analysis primarily to simplify representation of these results. The first few principal components, as usual, summarize the linear combinations of regional variables that account for the largest amounts of the total (genetic) covariance. More specifically, we can understand the first few PCs as representing anatomically distributed brain systems comprising regions that share major genetic effects on their variability. Since principal components are, by definition, mutually independent, it follows that the genetic effects shared by regions loading on the first PC are independent of the genetic effects shared by regions loading on the second (and subsequent) PCs. However, it does not follow that the development of a system defined by a single PC is under the control of a single gene or indeed that the genetic effects shared by regions loading on the first PC are determined by a unique set of genes that do not contribute to the genetic effects shared by regions on other PCs.

SUBJECTS AND METHODS

Sample Characteristics

Volunteer twin pairs were recruited from the community (Bartley *et al.*, 1997) and screened for a history of neurological, psychiatric, and other major medical illnesses. One member of a single MZ pair suffered a severe head injury due to a road traffic accident at age 7.5 years and was comatose for 6 weeks; the co-twin was involved in the accident but not injured. The sample consisted of 10 MZ pairs (6 male and 4 female pairs) of mean age 31 years (range 19–54 years) and 10 same-sex DZ pairs (4 male and 6 female pairs) of mean age 23 years (range 18–29 years). Note that the mean age of the MZ group is somewhat greater than that of the DZ group; however, this difference in means of 8 years is unlikely to have much differential impact on measures of brain structure in the two groups. Global gray matter volume decreases by approximately 0.7 mL/year on average over the age range 21–70 years (Pfefferbaum *et al.*, 1994).

The magnetic resonance study was approved by the NIMH Institutional Review Board and all volunteers gave informed consent in accordance with the Declaration of Helsinki.

MZ twins were identically matched for 19 red blood cell antigens. Population studies indicate that this pre-

dicts monozygosity at a conservative minimum 97% confidence level (Vogel and Motulsky, 1986). Information about chorion status was not available.

MRI Data Acquisition

Images were performed on a General Electric Signa 1.5 Tesla MR scanner with a T1-weighted spoiled GRASS sequence (repetition time = 24 ms, echo time = 5 ms); 124 contiguous sagittal slices 1.5 mm thick with an in-plane field of view of 240 mm across a 256×256 pixel matrix were acquired.

MRI Data Analysis

MR images were preprocessed using ANALYZE (Robb, 1989). Images were resized as 0.94-mm^3 voxels, rotated into axial orientation, and sectioned 2 mm below the inferior cerebellum. Minor artifacts in two images resulting from data storage errors were corrected at this stage by interpolation.

Preprocessed images were segmented into gray matter, white matter, cerebrospinal fluid (CSF), and skull/scalp compartments (with inhomogeneity correction) using SPM99b software (Friston *et al.*, 1995). Brain volumes were obtained in ANALYZE by (i) adding gray and white matter probability maps to estimate the proportion of parenchymal (non-CSF) tissue represented by each voxel, (ii) applying an intensity threshold to remove pixels with a low probability of representing either gray or white matter, and (iii) using a connectivity algorithm to remove extracerebral tissue. The segmentation failed on seven images (from five twin pairs) so for these pairs (10 subjects), cerebral volumes were obtained from the connectivity algorithm applied to brains stripped using "NIH Image" (Bartley *et al.*, 1997).

The lateral ventricles were extracted by manual segmentation of preprocessed images in ANALYZE. Lateral ventricular volumes (the sum of the two lateral ventricular volumes, but excluding third and fourth ventricular volumes) were obtained in ANALYZE by applying an intensity threshold and a connectivity algorithm to remove non-CSF pixels.

Preprocessed images were automatically transformed into Talairach space (Talairach and Tournoux, 1988) using SPM99b software (Friston *et al.*, 1995). This transformation was successful for all 40 images. The main motivation for anatomical normalization of these data was to allow an automated and entirely reliable regional parcellation of the brain.

A full description of the parcellation technique, including a figure of the parcellated template image and a complete list of the index coordinates defining each region in standard space, is given by Wright *et al.* (1999a). Briefly, the parcellation divided the cortex into a set of mutually exclusive volumes corresponding ap-

proximately to Brodmann's areas and divided subcortical gray matter into its main nuclei (e.g., thalamus) plus the cerebellum. This was done by first assigning one or more sets of index coordinates in the standard space of Talairach and Tournoux (1988) to each cerebral region based on the consensus view of the authors using the orthogonal slices of the Talairach atlas to identify regions. The three-dimensional Euclidean distances between a given voxel in the gray matter maps and the index coordinates for all (92) cerebral regions were computed, and that voxel was assigned to the region which had index coordinates closest to it (separated from it by the smallest Euclidean distance) over all sets of index coordinates in standard space. Regional gray matter densities were then calculated for each subject by dividing the sum of gray matter density over all voxels in a given region by the number of voxels that it contained.

The parcellation is validated by the prior results reported by Wright *et al.* (1999a), who applied this technique to measurement of gray matter and ventricular regional volumes in 27 patients with schizophrenia and 37 comparison subjects. Principal component analysis of these regional measurements demonstrated global and supraregional systems of anatomical covariation that were compatible with the known connectivity and function of the measured regions. Multiple univariate comparisons between these two groups also revealed a pattern of significant gray matter deficits in the patient group in lateral and medial temporal regions, insula, and inferior frontal and left dorsolateral prefrontal cortex. These gray matter changes were associated in patients with a significant excess of CSF ventricular volumes in several segments of the left lateral ventricle (Wright *et al.*, 1999a; Fig. 1). This pattern of anatomical abnormality in schizophrenia is largely corroborated by a meta-analysis of all relevant MRI studies published in the period 1988–1999 that used manual delineation to measure volumes of a few regions-of-interest in imaging data (Wright *et al.*, 2000).

In general, the convergence between anatomical regions parcellated solely on the basis of standard space coordinates (or by expert manual delineation of brain images) and the areas defined by Brodmann on the basis of microscopic examination of cortical cytoarchitectonics must be regarded as no more than approximate. As we have used the phrase in this paper, "Brodmann area" must therefore be understood as a convenient but approximate label for cortical regions and does not of course imply that our parcellation method is informed by cytoarchitectonic features. There has, however, already been some interesting early work to map cytoarchitectonically defined areas to a standard space coordinate system (Morosan *et al.*, 2001) and, in the future, it is possible to imagine that this approach might be generalized to provide more

sophisticated template images, which are truly informed by cytoarchitectonic and other microscopic neuroanatomical features, for automated regional parcellation of the whole brain.

Genetic Analysis

Brain volume and lateral ventricular volume: univariate analyses. The validity of the classical genetic analysis of an MZ/DZ twin study depends on a number of assumptions including (i) the trait variance is equal for MZ and DZ twins (which may be violated if, for example, factors operate on MZ but not on DZ pairs or if there is reciprocal twin interaction) and (ii) homoscedasticity, i.e., that the variation within a twin-pair is not related to the average of a pair (which may be violated if, for example, there is genotype-by-environment (GxE) interaction). We therefore also tested for unequal MZ/DZ variances and heteroscedasticity (Sham, 1998). Equality of MZ/DZ variances was tested by the F statistic, $F = (MST_{MZ})/(MST_{DZ})$, which has an F distribution (where MST is the total within-squares sum of squares for the measure) with $(2n_{MZ} - 1, 2n_{DZ} - 1)$ degrees of freedom under the hypothesis of equal variances. Homoscedasticity was tested using the Z test for heteroscedasticity (Sham, 1998). We then proceeded to path analysis using the Mx software package (Neale, 1997).

We first analyzed the brain volume and lateral ventricular volume data separately. In the univariate classical twin model, phenotypic variance is assumed to arise from the influence of four independent factors: A (additive genetic), D (dominance genetic), E (specific "nonshared" environment), and C (common "family" environment). Environment includes a wide range of nongenetic sources of variance from both the prenatal and the postnatal periods: common environmental effects might include the shared intrauterine environment; nonshared environmental effects might include a wide range of random variables including adult substance use or brain hydration at the time of scanning. Since our twin sample size was small, we had low power to detect dominance effects separately from additive genetic effects, and therefore we investigated only models with A, C, and E factors. The structural equation model for the phenotypic trait β of a twin can be written

$$\beta = aA + cC + eE, \quad (1)$$

where a , c , and e are the path coefficients of the model. In the twins of an MZ pair, the A and C factors are perfectly correlated and the E factors are uncorrelated. In the twins of a DZ pair, the C factors are perfectly correlated and E factors are uncorrelated; from genetic theory, the correlation between A factors is 0.5. The

path diagram for this model is shown in Fig. 1. The path coefficients a , c , and e were estimated by a maximum-likelihood method from the empirical covariance matrices for the MZ and DZ pairs for the variable β , and χ^2 measures of goodness-of-fit were calculated. The size of genetic effects can be assessed descriptively in terms of the heritability or proportion of total variance accounted for by additive genetic effects. For some analyses we have also reported 95% confidence intervals for the estimated heritability. A more formal approach is to test the hypothesis that the genetic effect (heritability) is zero, i.e., $a = 0$, or to test the hypothesis that the shared environmental effect is zero, i.e., $c = 0$, or to test the more general hypothesis that the genetic and shared environmental effects are both zero, i.e., $a = 0$ and $c = 0$ (Neale, 1997).

As the sample size was small, we had low power to test the hypotheses $a = 0$ or $c = 0$; false acceptance of these hypotheses can lead to overestimates of c and a , respectively (Christian *et al.*, 1995). Therefore we derived estimates for the a^2 , c^2 , and e^2 parameters, and their 95% confidence intervals, from the ACE model and used χ^2 tests of hierarchically nested models to test the hypotheses that both $a = 0$ and $c = 0$ (CE vs E models), $a = 0$ (ACE vs CE models), and $c = 0$ (ACE vs AE models).

Brain volume and lateral ventricular volume: bivariate analyses. We then analyzed brain volume and lateral ventricular volume data jointly to investigate whether there was an interrelationship in their genetic and environmental control. We fitted a common and specific factor model (Neale and Cardon, 1992). This assumes that there are common factors $A_c/C_c/E_c$ (assuming an ACE model) which affect both brain volume and lateral ventricular volume (Fig. 2). This model is not generally soluble without additional constraints. We therefore imposed the condition that the path parameter values (a_c, c_c, e_c) between $A_c/C_c/E_c$ and brain volume and between $A_c/C_c/E_c$ and lateral ventricular volume were equal (Loehlin, 1996).

Regional brain structure: multiple univariate and bivariate analyses. We applied genetic path analysis to the parcellated gray matter maps (46 left- and 46 right-sided gray matter regions). Since we were interested in regional genetic influences, we removed the potential confounding effect of global gray matter by regression. Thus, for each region, gray matter variables from the 40 subjects were regression. Thus, for each region, gray matter variables from the 40 subjects were regressed against global gray matter (the sum of the 92 regional gray matter values for each subject) and replaced by the standardized residuals of this regression.

First we applied univariate models (E, CE, AE, and ACE) to each region. We derived estimates for the a^2 ,

c^2 , and e^2 parameters from the ACE model and used χ^2 tests of nested models to test the hypotheses that both $a = 0$ and $c = 0$ (CE vs E models), $a = 0$ (ACE vs CE models), and $c = 0$ (ACE vs AE models).

Univariate models do not take into account the marked symmetry in brain structure. Therefore we also investigated bivariate models for bilateral brain regions (Fig. 2). First, we fitted a common and specific factor ACE model to each region (left and right sides) and derived path parameter estimates. We then tested the hypotheses that (i) there was no common genetic factor influencing regional brain measure variability ($a_c^2 = 0$) and (ii) genetic influences on right and left regional brain measure variability were equal ($a_{left}^2 = a_{right}^2$).

We have used a significance level of $P = 0.05$ for all hypothesis tests. This is justified principally by the exploratory nature of our analysis of a small- to moderate-sized sample. More definitive studies of larger samples might appropriately make corrections for multiple comparisons, although control of familywise type 1 error by a Bonferroni correction would be too severe in light of the correlated nature of the tests.

Genetic control and maturational stage. To investigate the hypothesis that ontogenetically early regions were more strongly predetermined than ontogenetically late regions (Lohmann *et al.*, 1999), we tested the Pearson coefficient of correlation between univariate heritability (a^2) and the typical gestational timing of gyral development of several brain regions (derived from Chi *et al.*, 1977); see Table 1.

Fluctuating asymmetry analyses: multiple univariate analyses. For each bilaterally homologous brain region, we tested the hypothesis that asymmetry variability was entirely under environmental control ($a = 0$ and $c = 0$ in an ACE model). We used a measure (S) of fluctuating asymmetry applied to global-corrected and standardized variables (where Y_{Li} is the left regional value for region Y in subject i , Y_{Ri} is the right regional value for region Y in subject i , Y_L is the left mean regional value for region Y over all 40 subjects, and Y_R is the right mean regional value for region Y over all 40 subjects). This measures the magnitude of the fluctuating asymmetry:

$$S_i = |Y_{Li} - Y_{Ri} - (Y_L - Y_R)| \quad (2)$$

The genetic and environmental influences on S were then estimated for each region by univariate genetic analysis (E, AE, CE, and ACE models).

Supraregional brain systems: genetic correlation matrix analysis. We investigated the patterns of genetic correlations between brain regions by principal component analysis. Using the standardized variables for the 92 gray matter regions (46 left and 46 right), we applied bivariate path analysis to all nonidentical pairs of

TABLE 1

Gestational Age at Time of First Sulcogyral Differentiation of Human Cortical Regions Labeled in Terms of Approximate Brodmann's Areas (after Chi *et al.*, 1977)

Brodman's area	Gestational age (weeks)
1	25
4	24
5	26
6	27
7	26
8	27
9	27
10	16
11	16
17	27
18	27
19	27
20	30
21	21
22	22
23	18
24	18
25	18
27	28
28	28
29	25
30	25
31	25
34	23
35	23
36	23
37	27
38	23
39	26
40	28
41	31
42	31
44	28
45	28
46	25
Insula	18

regions using a common and specific factor model (Fig. 2). From the bivariate path analyses, we calculated a genetic correlation (r_c) for each pair of brain regions, using the formula

$$r_G = a_c^2 / \sqrt{(a_{left}^2 + a_c^2)(a_{right}^2 + a_c^2)}. \quad (3)$$

We constructed a symmetric (92×92) genetic correlation matrix where each element represented the genetic correlation r_G between a pair of regions. We carried out principal components analysis on this matrix and extracted the first five eigenvectors. The loading of regions on these eigenvectors can be understood to identify distributed brain systems which share important effects on their heritability.

TABLE 2

Global Volumes of Brain and Ventricles for Each of 10 Monozygotic (MZ) and Dizygotic (DZ) Twin Pairs

Pair	Monozygotic twins				Dizygotic twins			
	Brain (cm ³)		Ventricles (cm ³)		Brain (cm ³)		Ventricles (cm ³)	
	A	B	A	B	A	B	A	B
1	1378	1374	9.6	9.6	1217	1218	11.4	5.7
2	1118	1169	6.7	13.6	1666	1519	17.0	13.8
3	1527	1557	14.4	7.3	1521	1433	24.7	22.7
4	1216	1163	26.4	12.9	1532	1266	6.6	5.2
5	1113	1103	21.0	15.1	1223	1314	16.8	11.0
6	1526	1554	27.9	21.6	1347	1146	11.0	7.8
7	1392	1390	10.7	11.0	1357	1279	3.3	4.9
8	1299	1377	15.2	13.6	1246	1311	12.6	17.4
9	1540	1472	24.9	13.9	1458	1473	4.6	13.7
10	1352	1523	61.4	23.9	1364	1450	21.8	15.1
Mean:	1357		18		1367		12	
SD:	161		12		135		6	

Note. MZ twin 10A has an unusually large ventricular volume, probably due to severe head injury in childhood, which accounts for the greater variability of ventricular volume in the MZ group.

RESULTS

Brain Volume and Lateral Ventricular Volume: Univariate Analyses

Brain volumes and lateral ventricular volumes for the 10 MZ and 10 DZ twin pairs are given in Table 2. There appeared to be an outlier for ventricular volume (twin 1, MZ pair 10) with a much larger volume (61.4 cm³) than all the other subjects. Interestingly this subject had a markedly lower cerebral volume than its pair (1352 cm³ vs 1523 cm³) and had suffered severe head injury in childhood. Male subjects had higher mean values for cerebral volume and lateral ventricular volume than female subjects (1445 cm³ vs 1279 cm³ and 18.9 cm³ vs 11.5 cm³, respectively).

The standard deviation for the MZ lateral ventricular volume (12 cm³) was markedly higher than that for the DZ lateral ventricular volume (6 cm³), violating the equal variance assumption for twin models ($F_{19,19} =$

3.53, $P = 0.004$). We therefore excluded MZ twin pair 10 (including the subject who had suffered severe head injury as a child and his uninjured co-twin) from the analyses, leaving 9 MZ pairs and 10 DZ pairs.

In addition, we standardized the cerebral volume and lateral ventricular volume variables (setting mean values to zero and variances to one), to facilitate comparison of the magnitude of the relative genetic and environmental influences on their variability. The descriptive statistics after these procedures are given in Table 3. In this sample, there was no evidence for unequal variances or heteroscedasticity in brain volume scores ($F_{17,19} = 1.33$, $P = 0.27$; $Z_{MZ} = 0.0$, $P = 0.5$, $Z_{DZ} = 0.15$, $P = 0.44$) or lateral ventricular volume scores ($F_{17,19} = 0.53$, $P = 0.83$; $Z_{MZ} = 0.55$, $P = 0.27$, $Z_{DZ} = 0.11$, $P = 0.46$).

For brain volume, path coefficients for the ACE model (Table 4) indicated that genetic factors contributed to the majority of variability ($a^2 = 0.66$), with

TABLE 3

Mean and Standard Deviation for Brain and Ventricular Volumes in Monozygotic and Dizygotic Twin Pairs

	Monozygotic twins		Dizygotic twins			
	Brain	Ventricles	Brain	Ventricles		
Estimated ("raw") variables (cm ³)						
Pairs 1–9	Mean:	1348	15	Pairs 1–10	1367	12
	SD:	165	6		135	6
Standardized variables						
Pairs 1–9	Mean:	-0.07	0.24	Pairs 1–10	0.06	-0.21
	SD:	1.11	0.99		0.91	0.98

Note. The data demonstrate that standard deviation of global volume measures is comparable between the two groups after removal of the outlier (and co-twin) from the MZ group.

TABLE 4

Results of Univariate Path Analysis, Fitting the ACE Model to Standardized Brain Volume and Ventricular Volume Separately Treated as Dependent Phenotypic Characteristics

	a ²	c ²	e ²	P(a = 0 and c = 0)	P(a = 0)	P(c = 0)
Brain volume (cm ³)	0.66 (0.17–1)	0.22 (0–0.94)	0.12 (0.06–0.25)	0.00	0.06	0.68
Baaré <i>et al.</i> (2001)	0.90 (0.85, 0.93)	0	0.10 (0.07, 0.015)		<0.001	NS
Ventricular volume (cm ³)	0.0 (0–0.53)	0.48 (0–0.97)	0.50 (0.32–0.84)	0.03	1.00	0.18
Baaré <i>et al.</i> (2001)	0	0.59 (0.47, 0.69)	0.41 (0.31, 0.53)		NS	0.025

Note. The squared path coefficients (a², c², e²) indicate the proportion of total variance in each measure that is attributable to additive genetic, common environmental, and nonshared environmental effects, respectively (95% confidence intervals are given parenthetically). The statistical significance of these effects can be gauged in terms of the probability of the data under the null hypothesis, assuming that one or more of the path coefficients is constrained to be zero. Thus the observed data are unlikely under the constraint that both the additive genetic effect and the common environmental effect are zero, i.e., P(a = 0 and c = 0) < 0.05 for both global volumes. However, the additive genetic effect seems larger for brain volume than for lateral ventricular volume. This conclusion is supported by comparable results from a much larger extended twin study by Baaré *et al.* (2001), which are also shown.

smaller contributions from common environment (c² = 0.22) and unique environment (e² = 0.12). These results were similar to those of Bartley *et al.* (1997) who analyzed this data set but with different techniques for cerebral volume measurement and genetic analysis.

For lateral ventricular volume, path coefficients for the ACE model (Table 4) indicated contributions from common environment (c² = 0.48) and unique environment (e² = 0.50) but not from genetic factors (a² = 0.0).

Brain Volume and Lateral Ventricular Volume: Bivariate Analyses

Cross-covariance matrices for MZ twin pairs 1–9 and DZ twin pairs 1–10 are given in Table 5. The overall fit of the common and specific factor model to these data was satisfactory (P = 0.99). The path coefficient estimates are given in Table 6. As shown also by the univariate results, brain volume was largely under genetic control (brain-specific heritability a² = 0.64) while lateral ventricular volume was largely under environmental control.

There was little evidence for common factors determining brain volume and lateral ventricular volume

variability, except for a small common shared environment effect (c_c² = 0.20).

Regional Brain Structure: Multiple Univariate and Bivariate Analyses

The results of univariate path analysis for the 46 bilateral brain regions are given in Table 7. There was evidence for a familial effect in 24 right-sided regions and 18 left-sided regions (null hypothesis that a = 0 and c = 0 rejected at 0.05 level). There was evidence for an additive genetic effect (null hypothesis that a = 0 rejected at 0.05 level) in two right-sided brain regions (precentral gyrus and anterior temporal pole) and in two left-sided brain regions (retrosplenial cortex and ventrolateral prefrontal cortex). There were 15 right-sided regions and 11 left-sided regions where the estimate for the additive genetic variability (a²) was greater than 0.5. This is displayed graphically in Fig. 3. No regions were found where there was evidence for a common environmental effect (null hypothesis that c = 0 rejected at 0.05 level).

The results of bivariate path analysis for the 46 bilateral brain regions are given in Table 8. This shows

TABLE 5

Cross-Covariance Matrices for Standardized Brain and Ventricular Volumes, Separately Estimated for Monozygotic (MZ) and Dizygotic (DZ) Twin Pairs

		A		B				A		B	
MZ		Brain	Ventricles	Brain	Ventricles	DZ		Brain	Ventricles	Brain	Ventricles
A	Brain	1.24				A	Brain	0.83			
	Ventricles	0.15	0.98				Ventricles	0.29	0.97		
B	Brain	1.12	0.07	1.24		B	Brain	0.41	0.25	0.83	
	Ventricles	0.07	0.30	0.15	0.98		Ventricles	0.25	0.63	0.29	0.97

Note. It is clear by inspection that twin-pair covariance of brain volume is greater for the MZ group than for the DZ group, whereas the twin-pair covariance of ventricular volume is greater for the DZ group than for the MZ group. For both groups, the covariance between brain and ventricular volumes is relatively small. Cross-covariance matrices in this form are used as the basis for bivariate path analysis; see Fig. 2 and Table 6.

TABLE 6

Results of Bivariate Path Analysis, Fitting the ACE Model to Standardized Brain Volume and Ventricular Volume Simultaneously Treated as Dependent Phenotypic Characteristics

Brain volume: specific factors			Common factors			Ventricular volume: specific factors		
a_b^2	c_b^2	e_b^2	a_c^2	c_c^2	e_c^2	a_v^2	c_v^2	e_v^2
0.64	0	0.05	0.03	0.20	0.06	0	0.26	0.43

Note. The total variance in brain volume is apportioned between six possible causes: genetic (a_b^2), common environmental (c_b^2), and nonshared environmental (e_b^2) effects specific to brain volume (rather than ventricular volume) and genetic (a_c^2), common environmental (c_c^2), and nonshared environmental effects (e_c^2) common to both brain and ventricular volume. Similarly, the total variance in ventricular volume is apportioned between specific and common causes. It is clear that the specific genetic effect on brain variability is large compared to the common genetic or environmental effects, which is consistent with inspection of the cross-covariance matrices (Table 5).

the parameter estimates for the common factors and unique right and left brain factors for those (14) regions where the estimated common heritability (a_{common}^2) was greater than 0.5. Of these, there were 7 regions where there was significant evidence for a shared genetic effect (Brodmann areas 24, 29, 31, 38, 41, 42, 47; null hypothesis that $a_c = 0$ rejected at 0.05 level). There was no region in which specifically left-sided and right-sided genetic effects were significantly different (null hypothesis that a_{left}^2 equal to a_{right}^2).

Genetic Control and Maturation Stage

The correlation between univariate heritability a^2 and developmental stage was -0.04 and this was not statistically significant ($P = 0.76$).

Fluctuating Asymmetry: Multiple Univariate Analyses

There were no regions where the estimated heritability of fluctuating asymmetry was greater than 0.5 and no evidence for significant familial, genetic, or common environmental effects on fluctuating asymmetry in any region.

Supraregional Brain Systems: Genetic Correlation Matrix Analysis

Brain regions loading positively on the first PC (15% total variance) included several frontal and parietal neocortical regions (including Brodmann areas 1, 4, 6, 7, 8, 9, 39, 40, 44, 46, 47); brain regions loading negatively on this PC included some limbic (right hippocampus) and paralimbic (anterior and posterior cingulate, left parahippocampus) regions (Table 9). We interpreted this PC as representing a frontoparietal–limbic/paralimbic genetic contrast.

Brain regions loading strongly on the second PC (9% total variance) included bilateral insula, lateral temporal cortex, and some frontal regions (Table 9). We interpreted this PC as representing a genetic system functionally related to audition.

The third, fourth, and fifth PCs (not shown) were not readily interpretable in terms of brain anatomy or functional systems.

DISCUSSION

In this study, we applied path analysis or structural equation modeling, informed by the classical twin model, to both global and regional neuroanatomical data to investigate the genetic control of human brain structure.

Our results need to be interpreted with regard to the limitations of the classical twin model (discussed by Bartley *et al.* (1997) and Phillips (1993)). Specifically, it is arguable that brain morphology in twins may be affected by an abnormal intrauterine environment with potential for low birth weight, prematurity, and other perinatal hazards. However, it seems unlikely that such environmental factors would be systematically confounded with zygosity, which is the basis for the path analysis reported here. It is also noteworthy that there was no history of major perinatal adversity in any of these subjects.

It is also important to be realistic, given the modest sample size of this study and the generally wide confidence intervals for path model parameter estimates, about our power to test statistical hypotheses. For this reason, we have presented the data descriptively and in the form of hypothesis tests. And when testing the significance of our model parameters we have adopted the recommendations of Christian *et al.* (1995) which are applicable to small studies of low power.

Brain Volume Variability

We found that brain volume variability was mainly under genetic control. However, our estimate for heritability ($a^2 = 0.66$) was lower than that of Bartley *et al.* (1997) ($a^2 = 0.94$), even though we analyzed the same data set. The difference in heritability estimates was mainly attributable to our use of the covariance matrix rather than the correlation matrix for structural equation modeling. Reanalysis of the Bartley *et al.* (1997) data, supplying a covariance matrix to Mx, gave $a^2 = 0.61$; the residual discrepancy probably reflects different segmentation processes and our exclusion of an outlying pair of MZ twins. There are theoretical reasons for preferring analysis of the covariance matrix to

TABLE 7
Results of Multiple Univariate Path Analyses

Region	Right cerebral hemisphere							Left cerebral hemisphere					
	BA	A ²	C ²	E ²	P(A&C = 0)	P(A = 0)	P(C = 0)	A ²	C ²	E ²	P(A&C = 0)	P(A = 0)	P(C = 0)
Postcentral gyrus	1, 2, 3	<u>0.30</u>	0.00	0.64	1.00	0.28	1.00	0.00	0.19	0.77	0.41	1.00	0.70
Precentral gyrus	4	<u>0.91</u>	0.00	0.17	<u>0.03</u>	<u>0.03</u>	1.00	0.00	0.44	0.52	<u>0.05</u>	1.00	0.32
Superior parietal lobule	5	<u>0.62</u>	0.00	0.43	<u>0.42</u>	<u>0.26</u>	1.00	0.12	0.00	0.82	<u>0.77</u>	0.75	1.00
Premotor cortex	6	<u>0.32</u>	<u>0.30</u>	<u>0.27</u>	<u>0.01</u>	<u>0.49</u>	<u>0.55</u>	<u>0.05</u>	<u>0.37</u>	<u>0.44</u>	<u>0.04</u>	<u>0.93</u>	<u>0.54</u>
Precuneus	7	<u>0.00</u>	<u>0.69</u>	<u>0.34</u>	<u>0.00</u>	1.00	0.09	<u>0.56</u>	<u>0.00</u>	<u>0.44</u>	<u>0.08</u>	<u>0.35</u>	1.00
Dorsolateral prefrontal cortex	8	<u>0.41</u>	<u>0.17</u>	<u>0.43</u>	<u>0.03</u>	<u>0.55</u>	<u>0.81</u>	<u>0.07</u>	<u>0.41</u>	<u>0.36</u>	<u>0.01</u>	<u>0.88</u>	<u>0.45</u>
Dorsolateral prefrontal cortex	9	0.00	0.00	1.03	1.00	1.00	1.00	0.18	0.00	0.78	0.61	0.70	1.00
Frontal pole	10	<u>0.51</u>	0.00	0.48	0.32	0.25	1.00	0.43	0.00	0.59	0.30	0.36	1.00
Orbitofrontal cortex	11	<u>0.54</u>	0.01	0.34	<u>0.02</u>	0.39	1.00	0.00	0.66	0.25	<u>0.00</u>	1.00	0.05
Orbitofrontal cortex	12	<u>0.08</u>	0.00	0.94	<u>0.83</u>	<u>0.89</u>	1.00	0.18	0.00	0.77	<u>0.77</u>	<u>0.56</u>	1.00
Visual cortex (V1)	17	0.00	0.09	0.88	1.00	0.70	0.74	0.00	0.40	0.57	0.07	1.00	0.15
Visual cortex (V2, V3)	18	0.21	0.49	0.25	<u>0.00</u>	0.60	0.30	0.00	0.48	0.48	<u>0.03</u>	1.00	0.26
Visual cortex	19	0.00	0.74	0.16	<u>0.00</u>	1.00	<u>0.04</u>	0.00	0.74	0.23	<u>0.00</u>	1.00	0.07
Inferior temporal gyrus	20	0.31	0.00	0.73	1.00	0.42	1.00	0.44	0.00	0.61	0.46	0.42	1.00
Middle temporal gyrus	21	0.00	0.25	0.76	0.30	1.00	0.59	0.00	0.27	0.75	0.27	1.00	0.38
Superior temporal gyrus	22	0.00	0.00	1.02	1.00	1.00	1.00	0.00	0.50	0.52	<u>0.03</u>	1.00	0.37
Posterior cingulate gyrus	23	<u>0.51</u>	0.00	0.37	0.17	0.23	1.00	<u>0.75</u>	0.00	0.18	<u>0.01</u>	<u>0.05</u>	1.00
Ant.-mid cingulate gyrus	24	<u>0.14</u>	0.34	0.51	<u>0.05</u>	0.84	0.58	<u>0.76</u>	0.14	0.13	<u>0.00</u>	<u>0.06</u>	0.78
Ant. cingulate gyrus	25	0.33	0.35	0.32	<u>0.01</u>	0.54	0.56	0.14	0.47	0.41	<u>0.01</u>	0.81	0.42
Retrosplenial cortex	27	0.22	0.00	0.80	1.00	0.49	1.00	0.00	0.00	1.02	1.00	1.00	1.00
Parahippocampal gyrus	28	0.10	0.17	0.73	0.33	0.91	0.80	0.43	0.00	0.54	0.26	0.36	1.00
Retrosplenial cortex	29	0.45	0.17	0.34	<u>0.02</u>	0.44	0.77	<u>0.84</u>	0.00	0.11	<u>0.01</u>	<u>0.01</u>	1.00
Retrosplenial cortex	30	0.00	0.69	0.34	<u>0.00</u>	1.00	0.15	<u>0.49</u>	0.00	0.51	0.09	0.42	1.00
Post cingulate gyrus	31	<u>0.60</u>	0.11	0.27	<u>0.01</u>	0.27	0.86	0.58	0.00	0.38	0.11	0.22	1.00
Medial frontal lobe	32	<u>0.00</u>	<u>0.53</u>	<u>0.32</u>	<u>0.00</u>	1.00	0.08	0.00	<u>0.53</u>	0.42	<u>0.01</u>	1.00	0.09
Temporal lobe (uncus)	34	0.00	0.64	0.39	<u>0.00</u>	1.00	0.07	0.00	<u>0.56</u>	0.44	<u>0.01</u>	1.00	0.15
Retrosplenial cortex	35	0.11	0.35	0.56	0.08	0.89	0.56	0.48	0.00	0.46	0.18	0.41	1.00
Occipitotemporal gyrus	36	0.00	0.00	1.02	1.00	1.00	1.00	0.31	0.00	0.69	0.51	0.38	1.00
Inf.-post temporal lobe	37	<u>0.58</u>	0.29	0.12	<u>0.00</u>	0.08	0.52	0.39	0.25	0.42	<u>0.05</u>	0.61	0.64
Ant. temporal pole	38	<u>1.00</u>	0.00	0.11	0.15	0.01	1.00	<u>0.80</u>	0.00	0.27	<u>0.03</u>	0.17	1.00
Angular gyrus	39	0.00	0.29	0.73	0.23	1.00	0.52	0.00	0.13	0.87	0.59	1.00	0.85
Supramarginal gyrus	40	<u>0.78</u>	0.00	0.23	<u>0.02</u>	0.10	1.00	0.30	0.00	0.72	0.37	0.49	1.00
Transverse temporal gyrus	41	0.49	0.24	0.29	<u>0.01</u>	0.37	0.68	<u>0.73</u>	0.02	0.30	<u>0.03</u>	0.25	0.97
Superior temporal gyrus	42	0.40	0.00	0.61	0.19	0.57	1.00	<u>0.72</u>	0.00	0.27	<u>0.02</u>	0.07	1.00
Inferior postcentral gyrus	43	<u>0.62</u>	0.00	0.46	0.31	0.23	1.00	0.00	0.00	1.02	1.00	1.00	1.00
Inferior frontal gyrus	44	0.38	0.19	0.45	0.04	0.59	0.77	0.08	0.36	0.59	0.09	0.92	0.55
Inferior frontal gyrus	45	0.00	0.07	0.94	0.76	1.00	0.81	0.00	0.04	0.95	1.00	0.87	0.87
Dorsolateral prefrontal cortex	46	0.00	0.49	0.52	<u>0.03</u>	1.00	0.32	0.00	0.00	0.96	1.00	1.00	1.00
Ventrolateral prefrontal cortex	47	0.34	0.00	0.59	0.55	0.26	1.00	<u>0.88</u>	0.00	0.24	0.17	0.04	1.00
Hippocampus	—	<u>0.71</u>	0.00	0.30	<u>0.05</u>	0.15	1.00	<u>0.66</u>	0.00	0.42	0.19	0.24	1.00
Thalamus	—	0.00	0.30	0.69	0.20	1.00	0.38	0.00	0.16	0.87	0.53	1.00	0.61
Corpus striatum	—	<u>0.60</u>	0.15	0.30	<u>0.02</u>	0.34	0.76	0.33	0.19	0.50	0.07	0.66	0.76
Putamen	—	<u>0.79</u>	0.00	0.31	<u>0.12</u>	0.11	1.00	0.09	0.47	0.47	<u>0.02</u>	0.89	0.40
Brain stem	—	<u>0.47</u>	0.00	0.41	<u>0.02</u>	0.55	1.00	0.38	0.00	0.53	0.12	0.44	1.00
Cerebellum	—	<u>0.67</u>	0.09	0.24	<u>0.01</u>	0.21	0.88	<u>0.66</u>	0.00	0.34	<u>0.05</u>	0.19	1.00
Insula	—	<u>0.80</u>	0.00	0.29	0.10	0.11	1.00	0.29	0.00	0.73	0.80	0.38	1.00

Note. Each row represents some key results of fitting the ACE path model to left and right homologous brain regions separately treated as dependent variables. As in Table 5, regions where the additive genetic effect on variance is important will have large heritability (regions with a² > 0.5 are underlined) and/or small probability under the null hypothesis that heritability is zero (regions with P(a = 0) < 0.05 or P(a = 0 and c = 0) < 0.05 are underlined). BA denotes approximate Brodmann's area.

the correlation matrix (Neale and Cardon, 1992). Our result is also comparable to the prior estimates by Todd *et al.* (1999) of 0.52 for heritability of total brain volume

(based on 63 female twin pairs), by Carmelli *et al.* (1999) of 0.81 for the heritability of intracranial volume (based on 85 elderly twin pairs), and by Baaré *et al.*

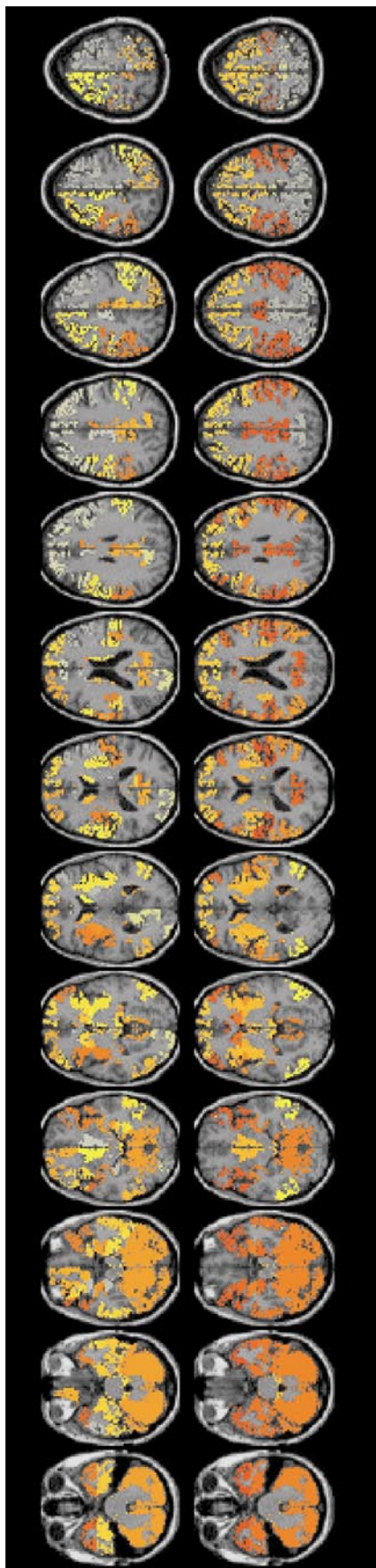


FIG. 3. Regional brain heritability maps. Top: gray matter regions with univariate heritability $a^2 > 0.5$ are colored pale yellow ($a^2 = 0.5$) to red ($a^2 = 1$) and superimposed on an axial MR image in standard space. Bottom: gray matter regions with symmetric heritability $a^2 > 0.5$ are colored according to the same color scale. Note that the most marked genetic effects on brain structure tend to be symmetrical and located in paralimbic, subcortical, and lateral temporal cortical structures.

(2001) of 0.90 for heritability of total brain volume; see Table 4. We conclude that brain volume seems heritable beyond doubt, but there is disagreement between studies concerning the precise proportion of total variance that is explained genetically. We have also shown that estimates of heritability and its standard error are conditional on various details of image processing and model fitting, particularly use of the covariance matrix rather than the correlation matrix in path analysis, which have differed between studies to date.

Ventricular Volume Variability

Although we found that there was a significant familial effect on lateral ventricular volume variability ($P = 0.03$), the parameter estimates ($a^2 = 0.00$ with 95% confidence interval 0.00–0.53, $c^2 = 0.48$, $e^2 = 0.50$) indicated that this effect was attributable to common environment rather than genetic factors. The size of the common environmental effect did not achieve statistical significance (null hypothesis $c = 0$; $P = 0.18$). In contrast, Reveley *et al.* (1982) measured ventricular areas in 11 monozygotic twin pairs and 8 dizygotic twin pairs and concluded that “ventricular area is under a very high degree of genetic control.” Their heritability estimates were not directly comparable to our estimates so we reanalyzed their data in Mx using their ventricular area correlations. By this technique, a^2 was 0.98, with 95% confidence interval [0.41, 1.00], again emphasizing that the width of confidence intervals for heritability estimates may be considerable in small- to moderate-sized twin studies. Carmelli *et al.* (1999) reported heritability of 0.65 for ventricular volume estimated in 85 elderly twin pairs. However, the results of another large recent study (Baaré *et al.*, 2001; see Table 4) are consistent with our findings that common environmental effects are the main source of familial covariation in ventricular volume and that the additive genetic effect is small, if not zero. Indeed Baaré *et al.* (2001) concluded that lateral ventricle volume was disqualified as a candidate endophenotype for genetic linkage studies because the evidence for any genetic effect on its structure was so slight. In this respect, it is interesting to recall the prior model of Cannon *et al.* (1989) that pathological variability of ventricular volume associated with schizophrenia was likely due to environmental factors such as perinatal trauma, whereas distributed gray matter deficit was genetically determined.

Regional Brain Variability

Our analysis of factors influencing regional brain variability demonstrated that there was significant evidence for a familial effect in multiple brain regions. In many of these regions, the parameter estimates indicated a major genetic effect, although this was signifi-

TABLE 8
Results of Multiple Bivariate Path Analyses

Region	BA	Common			Right specific			Left specific			P(A _c = 0)
		A ²	C ²	E ²	A ²	C ²	E ²	A ²	C ²	E ²	
Precentral gyrus	4	0.56	0.00	0.00	0.23	0.00	0.19	0.00	0.00	0.46	0.07
Post cingulate gyrus	23	0.57	0.00	0.09	0.00	0.00	0.25	0.09	0.00	0.12	0.08
Ant.-mid cingulate gyrus	24	0.73	0.00	0.00	0.00	0.00	0.34	0.00	0.12	0.12	<u>0.01</u>
Parahippocampal gyrus	28	0.55	0.00	0.06	0.00	0.00	0.42	0.00	0.00	0.37	0.15
Retrosplenial cortex	29	0.68	0.00	0.11	0.00	0.00	0.19	0.16	0.00	0.00	<u>0.03</u>
Post cingulate gyrus	31	0.58	0.00	0.00	0.03	0.09	0.27	0.00	0.00	0.38	<u>0.03</u>
Ant. temporal pole	38	0.85	0.00	0.00	0.05	0.00	0.15	0.00	0.00	0.29	<u>0.01</u>
Supramarginal gyrus	40	0.50	0.00	0.00	0.17	0.00	0.25	0.00	0.00	0.61	0.10
Transverse temporal gyrus	41	0.56	0.00	0.00	0.00	0.24	0.27	0.00	0.18	0.31	<u>0.03</u>
Superior temporal gyrus	42	0.58	0.00	0.00	0.00	0.00	0.50	0.14	0.00	0.26	<u>0.05</u>
Ventrolateral prefrontal cortex	47	0.59	0.00	0.02	0.00	0.00	0.45	0.12	0.00	0.27	<u>0.04</u>
Hippocampus	—	0.58	0.00	0.17	0.12	0.04	0.13	0.06	0.00	0.25	0.15
Corpus striatum	—	0.54	0.08	0.27	0.04	0.04	0.03	0.00	0.00	0.16	0.35
Cerebellum	—	0.63	0.00	0.22	0.12	0.00	0.02	0.00	0.00	0.14	0.22

Note. Each row represents some key results of fitting the ACE path model to left and right homologous brain regions simultaneously treated as dependent variables. Only brain regions where the common genetic heritability was large ($A_c^2 > 0.5$) are shown. $P(A_c = 0)$ denotes the probability of the data under the null hypothesis that the common genetic heritability is zero; BA denotes approximate Brodmann's area. (Regions with $P(A_c = 0) < 0.05$ are underlined).

icant for only a few regions. We investigated whether the strength of this genetic effect was related to maturational stage during neurodevelopment. Our model was derived from the study of Lohmann *et al.* (1999), who investigated sulcal variability in 19 pairs of monozygotic twins. Their results suggested that the shaping of deeper sulci was more strongly predetermined than that of superficial ones. They argued that this was likely to reflect the timing of gyral ontogenesis, where the deeper sulci are the first to appear, followed by the more shallow ones: the younger the sulcus, the stronger the influence of nongenetic factors. However, in our analysis, there was no correlation between the regional genetic parameter estimate (a^2) and the timing of gyral appearance. There are various possible explanations for this. First, although our hypothetical model (relating genetic control of variability and gyral ontogenesis) might be correct, a lack of correlation might result from inaccurate estimation of the genetic parameter (which is possible, since our sample size was small) or from a poor measure of regional maturation (we used the timing of gyral appearance during fetal development). Second, our assumption that regional gray matter volume is related to gyral patterning may be incorrect. The morphometric method that we have used depends on affine transformation of gray matter probability maps to match a template image in standard space. This technique does not coregister details of sulco-gyral anatomy, unlike some higher-order image registration algorithms (Thompson *et al.*, 1996), and so there will be an imperfect relationship between our regional volume measures and sulco-gyral markers of maturational stage.

This technical factor will have compromised our power to detect a relationship between genetic effects and maturational stage. Thus, although the hypothesis of an association between genetic determination and early ontogenesis was not supported by our results, there are several mitigating factors to consider in relation to its apparent refutation.

Bilateral Brain Regional Variability

We investigated whether variability in bilateral brain regions was under common genetic control. For 14 of the 46 regions, our parameter estimate for the common genetic factor was large ($a_c^2 > 0.5$), although this was significant for only 7 regions. These regions included multiple paralimbic regions and areas of temporal cortex functionally specialized for audition (Brodmann areas 41 and 42) where integration of bilateral sensory fields may be important.

We did not find evidence for a left/right difference in the genetic effects on variability in any of the 46 bilateral regions. In contrast, Tramo *et al.* (1995) measured regional cortical surface area for 32 bilateral regions and concluded that the left cerebral cortex was under stronger genetic control than the right. This was based on their finding that variation in regional surface area between unrelated twin pairs versus related twin pairs ("genotype effect") was significant for the left but not the right hemisphere. They suggested that there may be some link between greater genetic control of the left hemisphere, specialization of linguistic functions in the left hemisphere, and human evolution. Whether the differences between their findings and our findings are

TABLE 9
Principal Component (PC) Analysis of Genetic Correlation Matrix

BA	Region	Principal component 1		Principal component 2	
		Right	Left	Right	Left
1	Postcentral gyrus	0.19	0.13		
4	Precentral gyrus	0.12			
5	Superior parietal lobule	0.11	0.15		
6	Premotor cortex	0.16			
7	Precuneus		0.18		
8	Dorsolateral prefrontal cortex	0.17	0.10		-0.14
9	Dorsolateral prefrontal cortex	0.15			
10	Frontal pole				-0.13
11	Orbitofrontal cortex	0.13		0.16	0.12
12	Orbitofrontal cortex	-0.13			
18	Extrastriate cortex		0.14	0.20	
19	Extrastriate cortex		0.14		
20	Inferior temporal gyrus			0.18	0.22
21	Middle temporal gyrus	0.13			
22	Superior temporal gyrus			-0.10	-0.16
23	Post cingulate gyrus	-0.13	-0.15		
24	Ant.-mid cingulate gyrus	-0.12	-0.12		
25	Ant. cingulate gyrus		-0.10		
27	Retrosplenial cortex				0.10
28	Parahippocampal gyrus		-0.10		-0.15
29	Retrosplenial cortex	-0.13	-0.13		
30	Retrosplenial cortex		-0.13		
35	Retrosplenial cortex				-0.20
36	Occipitotemporal gyrus		0.18		
38	Ant. temporal pole	0.12		0.13	0.20
39	Angular gyrus	0.16	0.19		
40	Supramarginal gyrus	0.16	0.21		
41	Transverse temporal gyrus			-0.18	-0.19
42	Superior temporal gyrus			-0.22	-0.25
43	Inferior postcentral gyrus			0.11	
44	Inferior frontal gyrus	0.19	0.18		
45	Inferior frontal gyrus			-0.12	
46	Dorsolateral prefrontal cortex	0.13			
47	Ventrolateral prefrontal cortex	0.19	0.21		
—	Hippocampus	-0.10		0.11	
—	Putamen			0.24	0.22
—	Brain stem	-0.11	-0.12		
—	Cerebellum				0.18
—	Insula			-0.22	-0.23

Note. Anatomical regions loading on first and second principal components with eigenvector coefficients $> |0.1|$ are shown here. The first PC can be regarded as mainly a contrast between fronto-parietal neocortical structures and paralimbic/limbic structures; regions loading strongly on the second PC include several lateral temporal cortical structures specialized for audition. Brain regions loading strongly on the same PC share important effects on heritability.

accounted for by methodological differences, sample heterogeneity, or some other factor is not clear. However, our results suggest that further studies are required before accepting that there is greater genetic control of left than right regional brain structure.

Fluctuating Asymmetry

We did not find evidence for genetic control of fluctuating asymmetry. Fluctuating asymmetry refers to small and seemingly random left-right differences in symmetrical structures of an organism. Van Valen (1962) contrasted this with structures showing *directional asymmetry* (where there is normally a difference

in size of a structure on one side, e.g., the human heart) and *antisymmetry* (where there is normally an asymmetry induced by competitive interaction between the two sides, e.g., human handedness). Fluctuating asymmetry represents the failure of a developmental pathway on the two sides of an organism to be buffered against developmental noise. Molenaar *et al.* (1993) argued that epigenetic processes (rather than genetic or environmental processes) were the major source of developmental noise and represented the chaotic output of nonlinear deterministic systems. On this basis,

our failure to identify the genetic control of fluctuating asymmetry was expected and consistent with the results of other studies of heritability of fluctuating asymmetry in human anatomy, e.g. dental dimensions (Potter and Nance, 1976).

Genetic Correlation Matrix

Our analysis of the genetic correlation matrix for regional cerebral gray matter identified two supra-regional systems accounting for 24% of the total variance. We interpreted the first system as representing a frontoparietal–limbic/paralimbic genetic contrast and the second as a genetic system related to auditory functions. We postulate that the common genetic control of these two anatomical systems relates to two major processes in the evolution of the human brain: first the massive increase in size of the neocortex relative to archicortex/mesocortex and second the development of human language. In biomorphometric studies, the genetic correlation matrix has been used as a convenient description for the genetic structure of complex phenotypic traits, involving sets of interrelated quantitative characters that are polygenically inherited (Kingsolver and Wiernasz, 1991). In the field of evolutionary biology, it has been postulated that the genetic correlation matrix may reflect both developmental and functional interrelationships between characters (Turelli, 1988), resulting from the pleiotropic effects of gene action, although caution is required before inferring biological pleiotropism from statistical pleiotropism (Carey, 1988).

Methodological Issues

It is timely to reconsider some of the methodological issues arising from this study in relation to two comparable, recent imaging studies of brain heritability. The work by Baaré *et al.* (2001) is distinguished by its relatively large sample size (54 MZ and 58 DZ twins) and by an interesting extension of the classical twin design to include full siblings of twins (34 in total). These elements combine to the benefit of the statistical power of the study, which is estimated to have approximately 80% power to detect heritability of 70% or more (Posthuma and Boomsma, 2000). The study by Thompson *et al.* (2001), like the work reported here, involved 20 MZ and 20 DZ twins and is therefore relatively underpowered. The advantages of larger sample size are concretely demonstrated by the generally larger heritabilities, narrower confidence intervals, and more significant *P* values reported by Baaré *et al.* (2001); see Table 4. However, we have adopted a modeling strategy very similar to that of Baaré *et al.* (2001), using Mx software (Neale and Cardon, 1992; Neale, 1997) to estimate parameters of univariate and multivariate ACE models. In contrast, Thompson *et al.* (2001) used a simpler estimator of heritability (twice the difference

between MZ and DZ intraclass correlation coefficients), which did not entirely disambiguate additive genetic and common environmental sources of familial covariance. The choice of a simpler estimator of broad-sense heritability by Thompson *et al.* (2001) was motivated mainly by the relatively low degrees of freedom available to estimate parameters of more complex models, indicating that sample size may appropriately impact on model specification as well as statistical power. Similar considerations dictated our choice of an ACE model rather than the more complex ACDE model, which discriminates the effects of a dominant genetic (D) factor from an additive genetic (A) factor.

In addition to sample size and its ramifications, one other major point of difference between these studies is the anatomical resolution of genetic effects. Thompson *et al.* (2001) have pioneered the construction of genetic brain maps which localize broad-sense heritability in exquisite detail over the lateral cortical surface. They have also developed permutation tests to assess the significance of MZ–DZ differences in intraclass correlations and interregional (e.g., left–right) differences in heritability at each point on the cortical surface, with a minimum of distributional assumptions and strong type 1 error control (see Bullmore *et al.* (1999, 2001) and Nichols and Holmes (2002) for introductions to permutation testing in nongenetic brain mapping). The study by Baaré *et al.* (2001), on the other hand, resolves genetic effects anatomically only at the level of total gray and white matter volumes and lateral ventricular volume. Our study achieves an intermediate (regional) level of anatomical resolution which is unrefined and somewhat arbitrary compared to the voxel-level resolution of Thompson *et al.* (2001) but has the compensatory merit of being comprehensive. Specifically, we have estimated heritabilities of subcortical nuclei and paralimbic structures on the medial hemispheric surfaces (cingulate and parahippocampal gyri) which seem to express relatively strong genetic effects but are not addressed in the lateral cortical surface-based analysis of Thompson *et al.* (2001).

One future development to be anticipated on this basis is the application of comprehensive and voxel-level morphometric analyses to characterization of brain heritability in twin samples large enough for efficient estimation of genetic, environmental, and interactive effects.

CONCLUSIONS

There is major interest in using neuroimaging to understand genetic effects on human brain structure and function. In the post-genomic era, one feasible and promising strategy is to isolate genetic effects in terms of single polymorphisms (Egan *et al.*, 2001) but the classical twin design remains potentially informative about the relative importance of genetic effects com-

pared to nongenetic contributions to phenotypic variability. We have addressed some of the methodological issues arising in estimation of heritability at global, regional, and supraregional levels of human brain structure. We have confirmed some prior results that heritability of total brain volume is large compared to heritability of lateral ventricular volume, and at a finer level of anatomical resolution we have found that genetic effects on symmetric brain structure are more salient than genetic effects on asymmetric brain structure.

ACKNOWLEDGMENTS

We thank A. J. Bartley and D. W. Jones for their contribution to this study and X. Chitnis for methodological support. Dr. I. C. Wright and Professor E. T. Bullmore were supported by the Wellcome Trust.

REFERENCES

- Armstrong, E., Schleicher, H., Omran, H., Curtis, M., and Zilles, K. 1995. The ontogeny of human gyrification. *Cereb. Cortex* **5**: 56–63.
- Atchley, W. R., Rutledge, J. J., and Cowley, E. T. 1981. Genetic components of size and shape. II. Multivariate covariance patterns in the rat and mouse skull. *Evolution* **35**: 1037–1055.
- Baaré, W. F. C., Pol, H. E. H., Boomsma, D. I., Posthuma, D., de Geus, E. J. C., Schnack, H. G., van Haren, N. E. M., van Oel, C. J., and Kahn, R. S. 2001. Quantitative genetic modeling of variation in human brain morphology. *Cereb. Cortex* **11**: 816–824.
- Bartley, A. J., Jones, D. W., and Weinberger, D. R. 1997. Genetic variability of human brain size and cortical gyral patterns. *Brain* **120**: 257–269.
- Bertolino, A., Callicott, J. H., Elman, I., Mattay, V. S., Tedeschi, G., Frank, J. A., Breier, A., and Weinberger, D. R. 1998. Regionally specific neuronal pathology in untreated patients with schizophrenia: A proton magnetic resonance spectroscopic imaging study. *Biol. Psychiatry* **43**: 641–648.
- Bollen, K. A. 1989. *Structural Equations with Latent Variables*. Wiley, New York.
- Bullmore, E. T., Suckling, J., Overmeyer, S., Rabe-Hesketh, S., Taylor, E., and Brammer, M. J. 1999. Global, voxel and cluster tests, by theory and permutation, for a difference between two groups of structural MR images of the brain. *IEEE Trans. Med. Imag.* **18**: 32–42.
- Bullmore, E. T., Horwitz, B., Honey, G. D., Brammer, M. J., Williams, S. C. R., and Sharma, T. 2000. How good is good enough in path analysis of fMRI data? *NeuroImage* **11**: 289–301.
- Bullmore, E. T., Long, C. J., Suckling, J., Fadili, M. J., Calvert, G. A., Zelaya, F., Carpenter, T. A., and Brammer, M. J. 2001. Colored noise and computational inference in neurophysiological (fMRI) time series analysis: Resampling methods in time and wavelet domains. *Human Brain Mapp.* **12**: 61–78.
- Cannon, T. D., Mednick, S. A., and Parnas, J. 1989. Genetic and perinatal determinants of structural brain deficits in schizophrenia. *Arch. Gen. Psychiatry* **46**: 883–889.
- Carey, G. 1998. Inference about genetic correlations. *Behav. Genet.* **18**: 329–338.
- Carmelli, D., Sullivan, E. V., Swan, G. E., and Pfefferbaum, A. 1999. Evidence for heritability of brain structure in elderly male twins. *Mol. Psychiatry* **4**: 299.
- Cheverud, J. M. 1982. Phenotypic, genetic, and environmental morphological integration in the cranium. *Evolution* **36**: 499–516.
- Chi, J. G., Dooling, E. C., and Gilles, F. H. 1977. Gyral development of the human brain. *Ann. Neurol.* **1**: 86–93.
- Christian, J. C., Norton, J. A., Jr., Sorbel, J., and Williams, C. J. 1995. Comparison of analysis of variance and maximum likelihood based path analysis of twin data: Partitioning genetic and environmental sources of covariance. *Genet. Epidemiol.* **12**: 27–35.
- Dempsey, P. J., Townsend, G. C., Martin, N. G., and Neale, M. C. 1995. Genetic covariance structure of incisor crown size in twins. *J. Dental Res.* **74**: 1389–1398.
- Egan, M. F., Goldberg, T. E., Kolachana B. S., Callicott, J. H., Mazzanti, C. M., Straub, R. E., Goldman, D., and Weinberger, D. R. 2001. Effect of COMT Val (108/158) Met genotype on frontal lobe function and risk for schizophrenia. *Proc. Natl. Acad. Sci. USA* **98**: 6917–6922.
- Friston, K. J., Holmes, A. P., and Worsley, K. J. 1995. Statistical parametric maps in functional imaging: A general approach. *Human Brain Mapp.* **2**: 189–210.
- Jolliffe, I. T. 1986. *Principal Components Analysis*. Springer-Verlag, New York.
- Kieser, J. A. 1990. *Human Adult Odontometrics: The Study of Variation in Adult Tooth Size*. Cambridge Univ. Press, Cambridge, UK.
- Kingsolver, J. G., and Wiernasz, D. C. 1991. Development, function, and the quantitative genetics of wing melanin pattern in Pieris butterflies. *Evolution* **45**: 1480–1492.
- Loehlin, J. C. 1987. *Latent Variable Models: An Introduction to Factor, Path and Structural Analysis*. Erlbaum, Hillsdale, NJ.
- Loehlin, J. C. 1996. The Cholesky approach: A cautionary note. *Behav. Genet.* **26**: 65–69.
- Lohmann, G., von Cramon, D. Y., and Steinmetz, H. 1999. Sulcal variability of twins. *Cereb. Cortex* **9**: 754–763.
- Markow, T. A. 1992. Genetics and developmental stability: An integrative conjecture on aetiology and neurobiology of schizophrenia. *Psychol. Med.* **22**: 295–305.
- McGuffin, P., Asherson, P., Owen, M., and Farmer, A. 1994. The strength of the genetic effect: Is there room for an environmental influence in the aetiology of schizophrenia? *Br. J. Psychiatry* **164**: 593–599.
- Molenaar, P. C. M., Boomsma, D. I., and Dolan, C. V. 1993. A third source of developmental differences. *Behav. Genet.* **23**: 519–524.
- Morosan, P., Rademacher, J., Schleicher, A., Amunts, K., Schormann, T., and Zilles, K. 2001. Human primary auditory cortex: Cytoarchitectonic subdivisions and mapping into a spatial reference system. *NeuroImage* **13**: 684–701.
- Neale, M. C. 1997. *Mx: Statistical Modeling*. MCV, Richmond, VA.
- Neale, M. C., and Cardon, L. R. 1992. *Methodology for Genetic Studies of Twins and Families*. Kluwer Academic, Dordrecht.
- Nichols, T. E., and Holmes, A. P. 2002. Nonparametric permutation tests for functional neuroimaging: A primer with examples. *Human Brain Mapp.* **15**: 1–25.
- Olson, E., and Miller, R. 1958. *Morphological Integration*. Univ. of Chicago Press, Chicago.
- Pfefferbaum, A., Mathalon, D. H., Sullivan, E. V., Rawles, J. M., Zipursky, R. B., and Lim, K. O. 1994. A quantitative magnetic resonance imaging study of changes in brain morphology from infancy to late adulthood. *Arch. Neurol.* **51**: 874–887.
- Phillips, D. I. W. 1993. Twin studies in medical research: Can they tell us whether diseases are genetically determined? *Lancet* **341**, 1008–1009.
- Posthuma, D., and Boomsma, D. I. 2000. A note on the statistical power in extended twin designs. *Behav. Genet.* **30**: 147–158.
- Potter, R. H., and Nance, W. E. 1976. A twin study of dental dimension: I. Discordance, asymmetry and mirror imagery. *Am. J. Phys. Anthropol.* **44**: 391–396.

- Reveley, A. M., Reveley, M. A., Clifford, C. A., and Murray, R. M. 1982. Cerebral ventricular size in twins discordant for schizophrenia. *Lancet* **1**: 540–541.
- Robb, R. A., Hanson, D. P., Karwowski, R. A., Larson, A. G., Workman, E. L., and Stacy, M. C. 1989. ANALYZE—a comprehensive, operator-interactive software package for multidimensional medical image display and analysis. *Comput. Med. Imaging Graph.* **13**: 433–454.
- Sham, P. C. 1998. *Statistics in Human Genetics*. Arnold, London.
- Talairach, J., and Tournoux, P. 1988. *Co-Planar Stereotaxic Atlas of the Human Brain*. Thieme, Stuttgart.
- Thompson, P. M., Schwarz, C., Lin, R. T., Khan, A. A., and Toga, A. W. 1996. Three-dimensional analysis of sulcal variability in the human brain. *J. Neurosci.* **16**: 4261–4274.
- Thompson, P. M., Cannon, T. D., Narr, K. L., van Erp, T., Poutanen, V.-P., Huttunen, M., Lönquist, J., Standertskjöld-Nordenstam C.-G., Kaprio, J., Khaledy, M., Dail, R., Zoumalan, C. I., and Toga, A. W. 2001. Genetic influences on brain structure. *Nat. Neurosci.* **4**: 1253–1258.
- Todd, R. D., Health, A. C., Raichle, M. E., and Botteron, K. N. 1999. Heritability of human brain morphometry. *Mol. Psychiatry* **4**: 527–528.
- Tramo, N. J., Loftus, W. C., Thomas, C. E., Green, R. L., Mott, L. A., and Gazzaniga, M. S. 1995. Surface area of human cerebral cortex and its gross morphological subdivisions: In vivo measurements in monozygotic twins suggest differential hemisphere effects of genetic factors. *J. Cogn. Neurosci.* **7**: 292–301.
- Turelli, M. 1998. Phenotypic evolution, constant covariances, and the maintenance of additive variance. *Evolution* **42**: 1342–1347.
- Van Beijsterveldt, C. E. M., Molenaar, P. C. M., de Geus, E. J. C., and Boomsma, D. I. 1996. Heritability of human brain functioning as assessed by electroencephalography. *Am. J. Human Genet.* **58**: 562–573.
- Van Valen, L. 1962. A study of fluctuating asymmetry. *Evolution* **16**: 125–142.
- Vitt, L. J., Caldwell, J. P., Zani, P. A., and Titus, T. A. 1997. The role of habitat shift in the evolution of lizard morphology: Evidence from tropical *Tropidurus*. *Proc. Natl. Acad. Sci. USA* **94**: 3828–3832.
- Vogel, F., and Motulsky, A. G. 1986. *Human Genetics*. Springer-Verlag, Berlin.
- Waddington, C. H. 1940. Canalization of development and the inheritance of acquired characters. *Nature* **150**: 563–565.
- Weickert, C. S., and Weinberger, D. R. 1998. A candidate molecule approach to defining developmental pathology in schizophrenia. *Schizophrenia Bull.* **24**: 303–316.
- Weinberger, D. R., Berman, K. F., Suddath, R., and Torrey, E. F. 1992. Evidence of dysfunction of a prefrontal-limbic network in schizophrenia: A magnetic resonance imaging and regional cerebral blood flow study of discordant monozygotic twins. *Am. J. Psychiatry* **149**: 890–897.
- Wright, I. C., McGuire, P. K., Poline, J.-B., Travers, J., Murray, R. M., Frith, C. D., Frackowiak, R. S. J., and Friston, K. J. 1995. A voxel-based method for the statistical analysis of grey and white matter density in schizophrenia. *NeuroImage* **2**: 242–252.
- Wright, I. C., Sharma, T., Ellison, Z. R., McGuire, P. K., Friston, K. J., Brammer, M. J., Murray, R. M., and Bullmore, E. T. 1999a. Supra-regional brain systems and the neuropathology of schizophrenia. *Cereb. Cortex* **9**: 366–378.
- Wright, I. C., Ellison, Z. R., Sharma, T., Friston, K. J., Murray, R., and McGuire, P. K. 1999b. Mapping of gray matter changes in schizophrenia. *Schizophrenia Res.* **35**: 1–14.
- Wright, I. C., Rabe-Hesketh, S., Woodruff, P. W. R., David, A. S., Murray, R. M., and Bullmore, E. T. 2000. Meta-analysis of regional brain volumes in schizophrenia. *Am. J. Psychiatry* **157**: 16–25.